Laves-Phase Compounds of Alkaline Earths and Noble Metals

By Elizabeth A. Wood and Vera B. Compton

Bell Telephone Laboratories, Incorporated, Murray Hill, New Jersey, U.S.A.

The compounds $CaRh_2$, $CaPd_2$, $CaIr_2$, $CaPt_2$, $SrRh_2$, $SrPd_2$, $SrIr_2$, $SrPt_2$, $BaRh_2$, $BaPd_2$, and $BaPt_2$ are cubic Laves phases, $MgCu_2$ structure type (C15). This was determined by powder diffraction. The space group is O_h^7–$Fd3m$ with 8 formula weights in the unit cell.

For $BaPd_2$, $a_0 = 7.953$ Å; for $BaPt_2$, $a_0 = 7.920$ Å; for $BaRh_2$, $a_0 = 7.852$ Å; for $SrPd_2$, $a_0 = 7.826$ Å; for $SrPt_2$, $a_0 = 7.777$ Å; for $SrIr_2$, $a_0 = 7.700$ Å; for $SrRh_2$, $a_0 = 7.706$ Å; for $CaPd_2$, $a_0 = 7.665$ Å; for $CaPt_2$, $a_0 = 7.629$ Å; $CaIr_2$, $a_0 = 7.545$ Å; $CaRh_2$, $a_0 = 7.525$ Å.

The compounds $CaRh_2$, $CaPd_2$, $CaIr_2$, $CaPt_2$, $SrRh_2$, $SrPd_2$, $SrIr_2$, $SrPt_2$, $BaRh_2$, $BaPd_2$ and $BaPt_2$ were prepared and investigated for superconducting properties by Matthias & Corenzwit (1957). The rhodium and iridium compounds were superconducting but the platinum and palladium compounds were not.

These compounds had not been previously reported in the literature. However, after the present investigation was completed, Heumann & Kniepmeyer (1957) published a paper on the Laves phases in the strontium–palladium, –platinum, –rhodium, and –iridium systems. A comparison of their results with ours is included in this paper.

The procedure for preparation of the compounds described here was as follows. The alkaline earth metal was induction melted in an iron crucible and then

Table 1. *Comparison of calculated with observed intensities, visually estimated*

hkl	CaRh₂ Calc.	CaRh₂ Obs.	CaPd₂ Obs.	CaIr₂ Calc.	CaIr₂ Obs.	CaPt₂ Obs.	SrRh₂ Calc.	SrRh₂ Obs.	SrPd₂ Obs.	SrIr₂ Calc.	SrIr₂ Obs.	SrPt₂ Obs.	BaRh₂ Calc.	BaRh₂ Obs.	BaPd₂ Calc.	BaPd₂ Obs.	BaPt₂ Calc.	BaPt₂ Obs.
111	238	m–s	s	908	$vs.$	s	134	vw	m	579	s	s	8	Abs.	—	—	339	w
220	32	vw	vvw	33	Abs.	vvw	145	w	m	148	w–m	m	356	m	367	w	355	m[a]
311	412	s	vs	972	vvs	s	670	s	vvs	1384	vvs	vvs	1024	vs	1110	s	1937	s
222	292	m–s	s	850	vvs	s	318	m[h]	vs	912	vvs[b]	vs[g]	337	m	366	m–s	991	m–s
400	92	m	m	325	s	m	54	w	m	255	m–s[b]	m	29	Abs.	26	Abs.	197	w
331	55	m	m	223	s	m	20	vvw	vw	151	m	m	1	Abs.	2	Abs.	88	vw
422	10	Abs.	w	10	Abs.	Abs.	50	vw	m	58	Abs.	w–m	132	m	138	vw	134	w
511, 333	120	m–s	m–s	308	vs	m–s	203	m–s	vs	443	s	vs	314	s	339	m–s	624	m–s
440	118	m–s	m–s	313	vs	m–s	182	m–s	vs	423	s[b]	vs	261	s	280	m–s	559	m–s
531	40	w	w–m	160	m	m–s	15	vw	Abs.	108	m	s	1	Abs.	1	Abs.	63	w
620	4	Abs.	Abs.	4	Abs.	vvw	20	vw	w	20	Abs.	w	55	w	57	Abs.	58	w
533	42	m	m	106	w	m	70	w	m	152	m–s	vs[g]	110	m	118	w–m	219	m
622	104	m–s	m–s	313	vs	s	110	m	s	328	s[b]	vs	117	m	130	w–m	364	m–s
444	21	w	m	75	m	m	12	vvw	Abs.	57	m[b]	m	4	Abs.	6	Abs.	43	w
551, 711	24	w	m	96	m	m	10	Abs.	vvw	62	w	w–m	0.4	Abs.	0.8	Abs.	34	w
642	5	Abs.	Abs.	5	Abs.	vvw	28	Abs.	w	28	vw	w	74	w	74	vw	74	w
553, 731	97	s	s	239	vs	s	156	m	vs	327	s	vs	235	s	245	s	453	s
800	29	w	m	74	w–m	w	40	vw	w–m	91	m[b]	m	56	w	58	vw	118	w–m
733	12	vw	m	45	w	vw	4	Abs.	vvw	27	vw	w	1	Abs.	0.3	Abs.	14	vvw
660, 822	4	Abs.	Abs.	4	Abs.	Abs.	20	Abs.	w	21	vvw	w	52	w	52	vw	52	w
555, 751	87	s	s	213	m–s	s	126	m	s	268	s	vs	184	s	188	m	348	m
662	97	s	s	284	s	s	90	w	s	263	s	vs	87	w	92	w–m	258	m
840	72	m	m–s	279	s	s	36	vvw	m–s	168	m	s	9	Abs.	13	vvw	107	w
753, 911	49	m	m–s	187	s	s	15	Abs.	w	105	m	m–s	0.6	Abs.	1	Abs.	48	vvw
664	5	Abs.	Abs.	5	Abs.	Abs.	20	Abs.	w	20	Abs.	Abs.	47	vw	44	w	45	vvw
931	159	s	vs	377	vs	vs	176	m–s	vs	373	s	vs	225	s	213	m–s	411	m–s
844	—	—	vvs[c]	—	—	vvs[d]	428	vs	vvs	986	vs	vvs	428	vs	392	s	817	s
933, 771, 755	—	—	—	—	—	—	—	—	w–m[e]	—	—	s[f]	—	—	2	Abs.	90	vw
10,2,0, 862	—	—	—	—	—	—	—	—	—	—	—	—	—	—	363	m–s	439	w

a β line coincident.
b Ir line coincident.
c Calculated intensity is 375. Not observed in $CaRh_2$ and $CaIr_2$ because $\theta > 90°$.
d Calculated intensity is 1121.
e Calculated intensity is 39. Not observed in $SrRh_2$ and $SrIr_2$ because $\theta > 90°$.
f Calculated intensity is 270.
g Pt line coincident.
h Rh line coincident.

(vs = very strong; s = strong; m = medium; w = weak)

Table 2. *Observed interplanar spacings*

Values in Ångström units

hkl	CaRh₂*	CaRh₂	CaPd₂	CaIr₂	CaPt₂	SrRh₂	SrPd₂	SrIr₂	SrPt₂	BaRh₂	BaPd₂	BaPt₂
111	4·345	4·270	4·374	4·332	4·332	4·439	4·462	4·418	4·439	—	—	4·462
220	2·661	2·644	2·683	—	2·652	2·706	2·755	2·722	2·722	2·763	2·797	2·763
311	2·269	2·254	2·292	2·265	2·287	2·309	2·350	2·315	2·327	2·350	2·386	2·356
222	2·172	2·161	2·206	2·171	2·191	2·217	2·243	2·217[b]	2·232[e]	2·259	2·287	2·254
400	1·881	1·877	1·910	1·884	1·895	1·914	1·949	1·918[b]	1·933	—	—	1·961
331	1·726	1·719	1·755	1·728	1·746	1·746	1·791	1·765	1·774	—	—	1·804
422	1·536	—	1·561	—	—	1·570	1·593	—	1·588	1·603	1·621	1·610
511, 333	1·448	1·446	1·469	1·451	1·463	1·482	1·501	1·482	1·492	1·508	1·526	1·512
440	1·330	1·328	1·351	1·331	1·344	1·359	1·370	1·358[b]	1·372	1·388	1·400	1·389
531	1·272	1·271	1·293	1·269	1·287	1·301	—	1·301	1·312	—	—	1·331
620	1·190	—	—	—	1·199	1·217	1·234	—	1·228	1·238	—	1·259
533	1·148	1·146	1·166	1·148	1·161	1·173	1·191	1·174	1·182[e]	1·197	1·209	1·204
622	1·134	1·133	1·153	1·136	1·149	1·160	1·177	1·159[b]	1·170	1·183	1·194	1·187
444	1·086	1·085	1·103	1·088	1·099	1·111	—	1·108[b]	1·120	—	—	1·137
551, 711	1·054	1·052	1·072	1·056	1·066	—	1·093	1·077	1·087	—	—	1·105
642	1·006	—	—	—	1·017	—	1·045	1·028	1·037	1·049	1·059	1·057
553, 731	0·9797	0·9793	0·9962	0·9810	0·9917	1·003	1·018	1·002	1·011	1·022	1·033	1·028
800	0·9406	0·9405	0·9578	0·9422	0·9526	0·9621	0·9776	0·9615[b]	0·9706	0·9816	0·9926	0·9870
733	0·9194	0·9195	0·9389	0·9213	0·9308	—	0·9565	0·9399	0·9493	—	—	0·9646
660, 822	0·8869	—	—	—	—	—	0·9223	0·9070	0·9147	0·9261	0·9365	0·9321
555, 751	0·8689	0·8688	0·8844	0·8715	0·8802	0·8904	0·9030	0·8883	0·8975	0·9075	0·9176	0·9133
662	0·8632	0·8632	0·8786	0·8656	0·8747	0·8836	0·8973	0·8833	0·8913	0·9017	0·9120	0·9073
840	0·8413	0·8414	0·8567	0·8429	0·8524	0·8592	0·8755	0·8608	0·8690	—	0·8892	0·8841
753, 911	0·8260	0·8261	0·8409	0·8277	0·8367	—	0·8595	0·8449	0·8532	—	—	0·8676
664	0·8022	—	—	—	—	—	0·8341	—	—	0·8368	0·8472	0·8414
931	0·7889	0·7891	0·8032	0·7907	0·7994	0·8077	0·8202	0·8071	0·8149	0·8234	0·8334	0·8298
844	—	—	0·7822	—	0·7785	0·7865	0·7986	0·7857	0·7935	0·8015	0·8117	0·8085
933, 771, 755	—	—	—	—	—	—	0·7854	—	0·7816	—	—	0·7961
10,2,0, 862	—	—	—	—	—	—	—	—	—	—	0·7794	0·7765

Additional lines

CaRh₂		CaPd₂		CaIr₂		CaPt₂	
vw	2·103	w	3·480	vvs	2·212[b]	w	4·770
		m	2·475	vs	1·922[b]	w	3·079
		m	2·386[a]	vs	1·358[b]	vw	2·380[a]
		w	2·023	vs	1·157[b]	w–m	2·338
		w	1·692[a]	m	1·108[b]	w	1·981
		m	1·427	w–m	0·9590[b]	w	1·695
		w	1·386	vvs	0·8805[b]	w	1·667
				vvs	0·8579[b]	vw	1·305
				vvs	0·7836[b]		

SrPd₂		SrIr₂		SrPt₂		BaRh₂		BaPd₂		BaPt₂	
w	2·950[d]	vw	3·493	w	2·912	s	2·181[c]	w	2·232	vw	4·270
m	2·600[d]	s	0·8808[b]	m	2·146[f]	m–s	1·892[c]	w–m	2·062	w	3·351
w	2·475	s	0·8583[b]	s	2·058[d]	m–s	1·339[c]			vw	3·164
vw	1·821[d]	vs	0·7837[b]	w	1·957[e]	m–s	1·145[c]			m	2·495
vw	1·530			w	1·382[e]	w	1·098[c]			vw	1·473
w	0·8403			w	1·153[f]	w	0·9511[c]			w	1·453
				w	1·140	s	0·8716[c]			w	1·408
				vw	1·130[e]	s	0·8506[c]			w	1·011
				vw	1·074	vvs	0·7763[c]			w	0·9523
				w	0·9003[e]					w	0·9399
				m–s	0·8768[e]					w	0·8622
				vw	0·848						
				w–m	0·8005[e]						

[a] CaO, [b] Ir, [c] Rh, [d] SrO.8 H₂O, [e] Pt, [f] FePt

* Calculated values

allowed to cool. The noble metal was added to the crucible and the entire melt was reheated to a temperature somewhat above the melting point of the alkaline earth. The reaction was carried out in a helium atmosphere and the sample was then sealed in a glass tube to avoid oxide contamination.

X-ray diffraction powder photographs were taken of the resulting material, using a Norelco camera of 114·6 mm. diameter and Cu K radiation. The powder samples were contained in a thin-walled glass capillary in a nitrogen atmosphere.

The resulting patterns could be indexed on a cubic

lattice and were found, by comparison with the Frevel (1942) charts, to be very similar to that of $MgCu_2$. On the basis of this structure, relative intensities for each of the compounds were calculated, using the formula

$$I = p|F_{hkl}|^2 \frac{1+\cos^2 2\theta}{\sin^2 \theta \cos \theta} \times 10^{-5},$$

where p is the multiplicity factor, F_{hkl} the structure factor and the remaining term is twice the combined Lorentz and polarization factors. Thomas–Fermi scattering factors from the *International Tables* (1935) were used after applying dispersion corrections from Dauben & Templeton (1955). The results are given in Table 1 together with the visually estimated intensities. Since the scattering factors for palladium and rhodium and those for platinum and iridium are very similar, the intensities for $CaPd_2$, $CaPt_2$, $SrPd_2$ and $SrPt_2$ were not calculated. Instead the observed intensities for these compounds are compared with the calculated intensities for the corresponding rhodium or iridium compound.

The observed d values for the compounds are given in Table 2, together with the d values for the lines that do not belong to the $MgCu_2$ structure. Since the compounds are isomorphous, the d values were calculated only for $CaRh_2$ and are included in the table. All except the barium compounds gave sharp patterns, with separation of $K\alpha_1$ and $K\alpha_2$ lines usually beginning at $hkl = (731, 553)$.

The agreement between calculated and observed intensities in Table 1 is not perfect, but it is good. No major discrepancies occur and the minor ones may be due to superposition of impurity lines or preferred orientation. Absorption most probably accounts for the low intensity of the low-angle lines.

The intensities of reflections from different substances in Table 1 are not comparable with each other because of differences in exposure.

The product of the reaction between the alkaline earth and the noble metal was not pure in many cases. Some of the patterns included lines from the noble metal or from an oxide of the alkaline earth or both. In addition there were other lines which could not be indexed on the same lattice as the principal substance or any small multiple of it (i.e. not superlattice lines). In two patterns from a given sample the intensities of these lines differed relative to those of the principal substance. They indicate the presence of unidentified impurities. The chief impurities in the alloys according to spectrographic analyses are given below.

Alloy	Impurity (%)		
	Sr	Mg	Fe*
$CaRh_2$	—	0·01–0·3	—
$CaPd_2$	—	> 1	—
$CaIr_2$	—	—	—
$CaPt_2$	—	0·01–0·3	0·01–0·3
$SrRh_2$	—	0·01–0·3	—
$SrPd_2$	—	—	—
$SrIr_2$	—	0·01–0·3	—
$SrPt_2$	—	0·01–0·3	—
$BaRh_2$	0·01–0·3	—	—
$BaPd_2$	0·01–0·3	—	—
$BaPt_2$	0·01–0·3	0·01–0·3	0·01–0·3

* Very small amounts of iron (< 0·03%) were found in all the alloys, probably from reaction with the crucible.

The $MgCu_2$ structure, Type C15 (*Strukturbericht*, 1931), determined by Friauf (1927), is one of the structures commonly known as 'Laves phases' because Laves (1939, 1956) called attention to the special crystallographic interest of the A–A, B–B and A–B spatial relationships in these AB_2 compounds. The space group is O_h^7–$Fd3m$ with 8 formula weights in the unit cell. The A atoms occupy the positions of the diamond structure, (a) $0, 0, 0$; $\frac{1}{4}, \frac{1}{4}, \frac{1}{4}$; f.c., (Fig. 1(a)); the B atoms form a corner-sharing tetrahedral network, (d) $\frac{5}{8}, \frac{5}{8}, \frac{5}{8}$; $\frac{5}{8}, \frac{7}{8}, \frac{7}{8}$; $\frac{7}{8}, \frac{5}{8}, \frac{7}{8}$; $\frac{7}{8}, \frac{7}{8}, \frac{5}{8}$; f.c., (Fig. 1(b)). The five tetrahedra occupy the center and the four octants of the cubic cell unoccupied by A (Fig. 1(c)).

If the atoms are considered as hard spheres, the A atoms do not 'touch' the B atoms. As Schulze (1939) phrased it, if you set up a packing model of A atoms in the diamond structure, then center small balloons
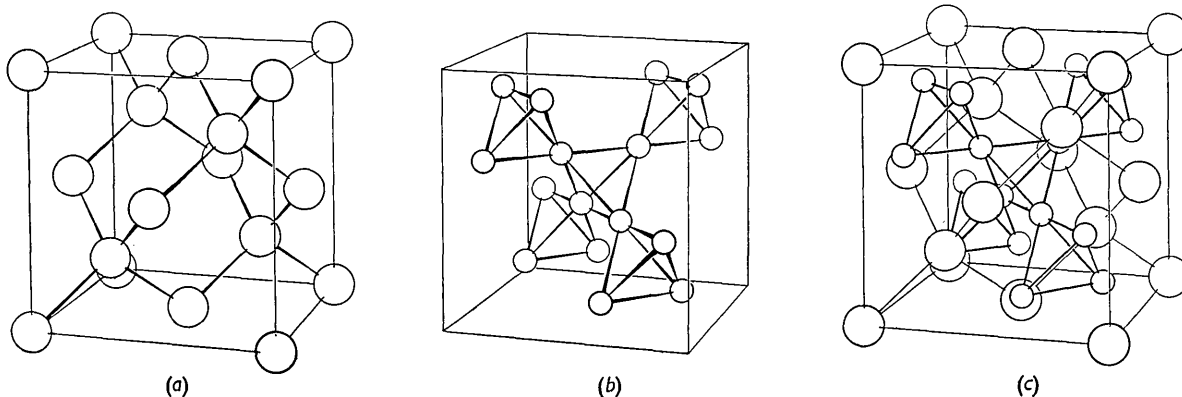

Fig. 1. The $MgCu_2$ structure. (a) A array (CN4), (b) B array (CN6), (c) AB_2 ($MgCu_2$) structure.

Table 3. *Radii*

Values in Ångström units

Atoms	AB_2	R_{CN12}	R_{CN6}	R_{CN4}	R_{Laves}	R_L-R_{CN12}	R_L-R_{CN6}	R_L-R_{CN4}
Ba		2·25		1·98				
	$BaPd_2$				1·72	−0·53		−0·26
	$BaPt_2$				1·71	−0·54		−0·27
	$BaIr_2$				—	—		—
	$BaRh_2$				1·70	−0·55		−0·28
Sr		2·16		1·90				
	$SrPd_2$				1·69	−0·47		−0·21
	$SrPt_2$				1·68	−0·48		−0·22
	$SrIr_2$				1·67	−0·49		−0·23
	$SrRh_2$				1·67	−0·49		−0·23
Ca		1·97		1·73				
	$CaPd_2$				1·66	−0·31		−0·07
	$CaPt_2$				1·65	−0·32		−0·08
	$CaIr_2$				1·63	−0·34		−0·10
	$CaRh_2$				1·63	−0·34		−0·10
Pd		1·37	1·30					
	$BaPd_2$				1·41	+0·04	+0·11	
	$SrPd_2$				1·38	+0·01	+0·08	
	$CaPd_2$				1·36	−0·01	+0·06	
Pt		1·38	1·31					
	$BaPt_2$				1·40	+0·02	+0·09	
	$SrPt_2$				1·38	0·00	+0·07	
	$CaPt_2$				1·35	−0·03	+0·04	
Ir		1·35	1·28					
	$BaIr_2$				—	—	—	
	$SrIr_2$				1·36	+0·01	+0·08	
	$CaIr_2$				1·34	−0·01	+0·06	
Rh		1·34	1·27					
	$BaRh_2$				1·39	+0·05	+0·12	
	$SrRh_2$				1·36	+0·02	+0·09	
	$CaRh_2$				1·33	−0·01	+0·06	

on the B sites and let them swell uniformly until they touch each other, they will not yet touch the A atoms (see Fig. 2). Examination of Fig. 2 shows that the
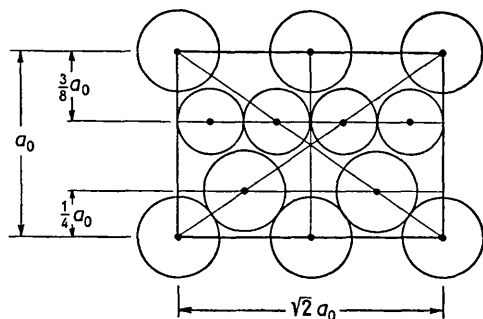

Fig. 2. The (110) section through a packing model of the $MgCu_2$ structure. Larger atoms are A atoms; smaller atoms are B atoms.

shortest A–A distance is $(\sqrt{3})/4a_0$ and the shortest B–B distance is $(\sqrt{2})/4a_0$. The radius ratio R_A/R_B in this structure is therefore $\sqrt{3}/\sqrt{2}$, if the radius of each atom is considered to be half the distance between centers of nearest like atoms, as in Fig. 2. The radii, so calculated, for the atoms in the compounds here reported are given in Table 3, which also lists the CN12, CN6 and CN4 radii for comparison. The CN12 radii are taken from Laves' (1956) paper and the CN4

and CN6 radii are calculated by use of Laves' (1956) correction curve.

The CN4 and CN12 radii are given for the A atoms each of which is coordinated to four A atoms at $0·433a_0$ ($= (\sqrt{3})/4a_0$) and to twelve B atoms at $0·415a_0$ ($= (\sqrt{11})/8a_0$). The CN6 and CN12 radii are given for the B atoms each of which is coordinated to six B atoms at $0·354a_0$($= (\sqrt{2})/4a_0$) and to six A atoms at $0·415a_0$ ($= (\sqrt{11})/8a_0$).

In Table 3, comparison of the radius of the A atom in the Laves phase with either its CN12 or CN4 radius shows the Laves-phase A radius to be appreciably smaller in all cases, whereas the Laves-phase B radius is larger than the CN6 radius of B in all cases and larger than the CN12 radius in nearly all cases, the exceptions showing zero or very small negative differences.

Thus in general, the alkaline earth atoms have contracted and the noble metals have expanded to form this structure. On the basis of a hard-sphere model, the alkaline earth atoms (A) might be expected to determine the lattice constant. The data in Table 4

Table 4. *Lattice constants*

Values in Ångström units

	Pd	Pt	Ir	Rh
Ba	7·953±0·005	7·920±0·005	—	7·852±0·005
Sr	7·826±0·005	7·777±0·005	7·700±0·005	7·706±0·005
Ca	7·665±0·005	7·629±0·005	7·545±0·005	7·525±0·005

show that in fact the lattice constant varies significantly when the noble metal atom (B) is changed.

The lattice constants of the Pd and Pt compounds indicate that the effective radius for Pd in these compounds is larger than that for Pt. Heumann & Kniepmeyer's (1957) data are also in agreement with this conclusion. However, the lattice constants given by Heumann & Kniepmeyer for the strontium compounds do not agree with those published here within our limits of error. They give the following values:

$$SrPd_2, \ 7\cdot800 \ \text{Å} \ (\varDelta = +0\cdot026);$$
$$SrPt_2, \ 7\cdot742 \ \text{Å} \ (\varDelta = +0\cdot035);$$
$$SrRh_2, \ 7\cdot695 \ \text{Å} \ (\varDelta = +0\cdot011);$$
$$SrIr_2, \ 7\cdot849 \ \text{Å} \ (\varDelta = -0\cdot149) \ .$$

Heumann & Kniepmeyer give the experimental data for one substance, $SrRh_2$. When the lattice constant for $SrRh_2$ is determined from their data by Bradley–Jay extrapolation, the result is $7\cdot707\pm0\cdot005$ Å, which agrees with our lattice constant, similarly determined, within experimental error. This difference in treatment of data may well account for the discrepancy between their results and ours in the cases of $SrPd_2$ and $SrPt_2$ as well, but may not account for the different results for $SrIr_2$. The larger discrepancy in this case might be due to impurity or off-stoichiometry of material. The results of the spectroscopic analyses of our material and the chemical analyses of their material preclude the presence of appreciable amounts of metallic impurities, but non-metallic impurities would not have been detected by the spectroscopic analysis. While departure from stoichiometry would have been possible in both cases, it seems unlikely in this structure that one of the constituents would substitute for the other because of the great difference in size and bonding of the two constituents. Vacancies, however, could occur.

References

DAUBEN, C. H. & TEMPLETON, D. H. (1955). *A Table of Dispersion Corrections for X-Ray Scattering of Atoms.* University of California Radiation Laboratory UCRL-3061.

FREVEL, L. K. (1942). *Industr. Engng. Chem. Anal. Ed.* **14**, 687.

FRIAUF, J. B. (1927). *J. Amer. Chem. Soc.* **49**, 3107.

HEUMANN, TH. & KNIEPMEYER, M. (1957). *Z. anorg. Chem.* **290**, 191.

International Tables for the Determination of Crystal Structures (1935). Berlin: Borntraeger.

LAVES, F. (1939). *Naturwissenschaften,* **27**, 65.

LAVES, F. (1956). *Theory of Alloy Phases.* Cleveland: American Society of Metals.

MATTHIAS, B. T. & CORENZWIT, E. (1957). *Phys. Rev.* **107**, 1558.

SCHULZE, G. E. R. (1939). *Z. Elektrochem.* **45**, 849.

A Guide Mechanism for a Single-Crystal X-ray Counter Goniometer

BY A. McL. MATHIESON

Chemical Physics Section, Division of Industrial Chemistry, Commonwealth Scientific and Industrial Research Organization, Melbourne, Australia

A mechanism has been devised which permits the counter on a X-ray goniometer to scan a selected straight line in reciprocal space within the range of the limiting sphere.

Introduction

A counter goniometer offers the possibility of increased sensitivity and accuracy in intensity measurements on single crystals, a possibility which can best be adequately exploited if the goniometer is made automatic in operation. In the design of such a goniometer, the principal disadvantage of the counter is that it is a one-point detector, so that the conditions governing its orientation with respect to the crystal to record a sequence of reflexions are much more critical than those required by a goniometer employing photographic film, i.e., a two-dimensional detector.

In the majority of cases, the problem of satisfying the required conditions has been tackled by hand-setting both the crystal and the counter (see Lonsdale (1948), Wooster, Ramachandran & Lang (1948), Cochran (1950), Clifton, Filler & McLachlan (1951), Evans (1953), Zachariasen (1954), Furnas & Harker (1955)). To make the collection of intensity measurements automatic, it is necessary to devise a linkage between the crystal and counter movements which will enable the whole or a selected part of the recip-